

ApproxABFT: Approximate Algorithm-Based Fault Tolerance for Vision Transformers

Xinghua Xue, Cheng Liu, Haitong Huang, Bo Liu, Ying Wang, Bing Yang, Tao Luo, Lei Zhang, Huawei Li, Xiaowei Li

Abstract—Vision Transformers (ViTs) with outstanding performance becomes a popular backbone of deep learning models for the main-stream vision tasks including classification, object detection, and segmentation. Other than the performance, reliability is also a critical metric for the adoption of ViTs in safety-critical applications such as autonomous driving and robotics. With the observation that the major computing blocks in ViTs such as multi-head attention and feed forward are usually performed with general matrix multiplication (GEMM), we propose a classical algorithm-based fault tolerance (ABFT) strategy originally developed for GEMM to protect ViTs against soft errors in the underlying computing engines. Unlike classical ABFT that will invoke the expensive error recovery procedure whenever computing errors are detected, we leverage the inherent fault-tolerance of ViTs and propose an approximate ABFT, namely ApproxABFT, to invoke the error recovery procedure only when the computing errors are significant enough, which skips many useless error recovery procedures and simplifies the overall GEMM error recovery. Meanwhile, it also relaxes the error threshold in error recovery procedure and ignores minor computing errors, which reduces the error recovery complexity and improves the error recovery quality. In addition, we also apply a fine-grained blocking strategy to ApproxABFT and split GEMM with distinct sizes into smaller sub blocks such that it can smooth the error thresholds across ViTs and further improve the error recovery quality. According to our experiments, the ApproxABFT reduces the computing overhead by 25.92% to 81.62% and improves the model accuracy by 2.63% to 72.56% compared to the baseline ABFT while the blocking optimization further reduces the computing overhead by 6.56% to 73.5% with comparable accuracy.

Index Terms—ABFT, Fault-Tolerant Deep Learning, Vision Transformers, Approximate

I. INTRODUCTION

Vision transformers (ViTs) [1]–[3] with outstanding performance over convolutional neural networks (CNNs) [4] in the main-stream vision tasks including objection detection [5] [6] and classification [7] [8] attract a lot of research efforts from both academia and industry recently. Many ViTs [9] have been applied in safety-critical applications such as autonomous driving. It can be envisioned that the trend will continue and reliability will be a critical metric that determines the adoption of ViTs in these applications. ViTs with intensive computing can incur considerable overhead when protected

Corresponding author: Cheng Liu.

The authors are with the State Key Lab of Processors, Institute of Computing Technology, Chinese Academy of Sciences, Beijing 100190, China, and also with the University of Chinese Academy of Sciences, Beijing 100190, China (e-mail: {xuexinghua, liucheng}@ict.ac.cn)

with conventional fault-tolerant approaches such as triple modular redundancy [10] [11] and recomputing [12] [13].

Fortunately, we notice that the major computing kernels in ViTs such as multi-head attention (MHA) and feed forward (FF) are usually implemented with general matrix-matrix multiplication (GEMM), which can be protected using classical algorithm-based fault tolerance (ABFT) [14] strategy based on checksum with much less computing overhead compared to redundancy and recomputing. ABFT has been successfully adopted in many applications like FFT [15] and CNNs [16] [17] for both higher reliability and less computing overhead. Inspired by prior works, we mainly explore the use of ABFT for fault-tolerant ViTs in this work.

To begin, we introduce the basis of ABFT with an example as shown in Fig.1. First of all, it calculates row sum and column sum of the two input matrices respectively and utilizes the two sum vectors to calculate output matrix sum with dot product. By checking the calculated matrix sum with that obtained with output matrix, output matrices with errors can be detected. When computing errors are confirmed, error recovery procedure will be invoked. Error recovery can be split into sum calculation, error localization, and error correction. In sum calculation, row sum and column sum of the output matrix are calculated with two matrix-vector multiplication respectively. In error localization, we can identify if there are computing errors in a row or a column by checking the row sum or column sum similar to the error detection, and determine the possible faulty elements as shown in the right side of Fig. 1. In error correction, an error can be corrected by adding the sum deviation to the faulty element only when there is a single computing error in a row or column. Otherwise, the computing errors cannot be corrected. Many ABFT implementations may just ignore them or recompute the faulty elements.

Basically, ABFT error recovery starts only when error is detected. Suppose the matrix size is $n \times n$, error detection mainly requires a vector dot product and incurs n MACs while error recovery is more expensive and it requires two matrix-vector multiplication with $2 \times n^2$ MACs. Error recovery will be frequently invoked when there are many computing errors at higher error rate. On the other hand, the fault tolerance capability of ABFT is limited and ABFT fails when there are multiple errors in the same row and column at higher error rate. As a result, the ABFT computing overhead can increase dramatically without effective fault recovery at higher BER.

Existing ABFT works [18]–[20] mainly optimized the

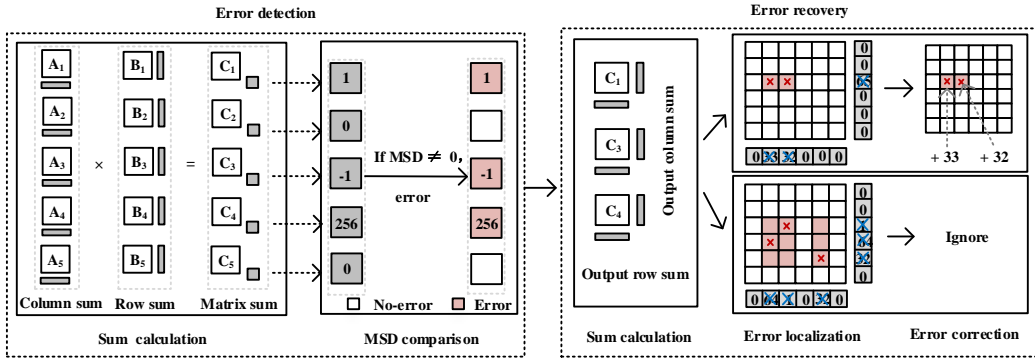


Fig. 1. A baseline ABFT for GEMM mainly consists of an error detection procedure and an error recovery procedure.

ABFT implementation for higher performance or less computing overhead. For instance, [18] presented a design of a high-performance GPU-based GEMM that integrated an algorithm-based fault tolerance scheme and explored fused ABFT schemes for GEMM with respect to the thread level, warp level, and threadblock level. [19] proposed four ABFT schemes including full checksum, column checksum, row checksum and checksum-of-checksum to protect the convolutional layers against soft errors, and designed a multi-scheme workflow for soft error protection with layerwise optimization to obtain high detection/correction capability with limited runtime overhead. However, the kernel of different ABFT implementations still rely on accurate checksum based comparison. In addition, they mostly target GEMMs and CNNs, and there is still a lack of investigation of ABFT for ViTs.

We notice that the major computing kernels in ViTs are usually resilient to soft errors and can tolerate many minor computing errors as shown in Section II. With this observation, we propose an approximate ABFT approach, namely Approx-ABFT, which leverages the inherent fault tolerance of ViTs to relax the error detection and error recovery metrics in classical ABFT for less computing overhead and higher model accuracy. For the error detection, we raise the error detection threshold such that many minor computing errors can be ignored and expensive fault recovery procedures can be avoided without compromising the model accuracy. For the error recovery, we also set higher error thresholds for the error localization, which can potentially reduce the number of faulty elements and simplify the error correction. In addition, we investigate how to handle the uncorrectable faulty elements such that they pose less negative influence on the model accuracy. Moreover, we also apply a blocking strategy to split the GEMMs in ViTs into smaller sub GEMMs and avoid distinct approximation thresholds to handle different ViT layers and GEMMs across ViTs. With approximate blocking setups, the block-wise ApproxABFT can achieve higher accuracy with less computing overhead. According to our experiments, the proposed ApproxABFT shows clear model accuracy improvement and less computing overhead at the same time compared to the classical ABFT. The contributions are summarized as follows.

- We investigated the fault tolerance of ViTs and analyzed

the computing deviation distribution induced by soft errors for the first time. We observe that the soft error induced deviations of matrix sum and row/column sum vary substantially across the GEMMs in ViTs but exhibit similar trend. In addition, most of the deviations are small and has little influence on the model accuracy.

- We propose an approximate ABFT (ApproxABFT) to relax the error detection and error recovery in classical ABFT such that expensive error recovery can be reduced and some of the uncorrectable computing errors can be approximated with less accuracy penalty.
- We also investigate the influence of fine-grained blocking setups on ApproxABFT and simplify the implementation of ApproxABFT by utilizing the same thresholds across all the sub GEMMs.
- According to our experiments, ApproxABFT reduces the computing overhead by 25.92% to 81.62% and improves the model accuracy by 2.63% to 72.56% compared to the baseline ABFT. With optimized blocking strategy, the computing overhead can be further reduced by 6.56% to 73.5% with comparable accuracy.

II. MOTIVATION

In this section, we explore the correlation between computing errors and model accuracy in presence of soft errors and investigate the fault tolerance capability of ViTs. Then, we brief challenges of using ABFT for protecting ViTs.

We take DeepViT-S on ImageNet as an example and the Top-1 accuracy as the accuracy metric. We utilize bit error rate (BER) to represent the bit flip error intensity and conduct the reliability analysis based on an operation-wise fault injection platform which injects random bit flip errors to outputs of the primitive operations such as addition and multiplication [21]. Then, we compare the accuracy with the different computing error metrics of the model. Specifically, we utilize output matrix sum deviation (MSD) and row/column sum deviation (R/CSD) to characterize the bit flip errors induced computing deviations. The comparison in Fig.2(a) reveals the correlation between MSD and model accuracy. Fig.2(b) reveals the correlation between R/CSD and model accuracy. L1, L9, and L16 denote the first, ninth, and sixteenth layers in the model, respectively. In general, MSD, R/CSD, and the model accuracy

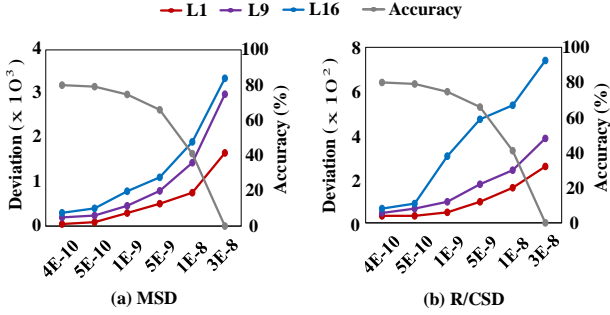


Fig. 2. Correlation between DeepViT-S accuracy and computing deviation of matrix sum and row/column sum i.e. MSD and R/CSD.

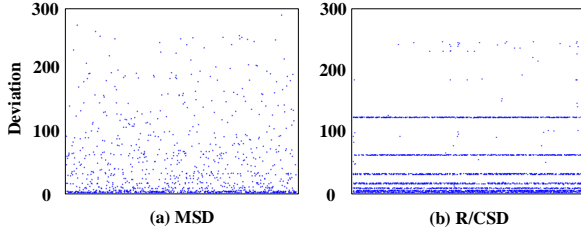


Fig. 3. MSD and R/CSD of the largest output matrix in each DeepViT-S layer when BER is 5E-10.

are roughly monolithic to BER and exhibit consistent trend in general despite the distinct values. Thereby, we can leverage MSD or R/CSD as indicators to predict the model accuracy. For instance, when MSD is less than 100, we can predict that the accuracy of DeepViT-S can be close to that of clean DeepViT-S. Similar predictions can also be obtained based on R/CSD.

To gain insight of the different computing deviations, we set BER to be 5E-10 when the model accuracy just starts to drop and present the statistic of MSD and R/CSD of the largest output matrix in each DeepViT-S layer. The result as shown in Fig. 3 demonstrates that the majority of the MSD is close to zero and pose negligible influence on the model accuracy according to the correlation between accuracy and MSD. Similar to MSD, the majority of R/CSD is also close to zero and can be ignored, but R/CSD also include quite some of the data clustered at relatively larger values, which may depend on data value distribution at specific rows or columns.

As mentioned, ABFT has limited fault tolerance capability and cannot recover GEMMs with multiple computing errors in the same row and column. The percentage of rows and columns with multiple computing errors that cannot be recovered in DeepViT-S is presented in Fig. 4. It demonstrates that the percentage of computing errors that cannot be recovered with ABFT grows rapidly with the increase of BER. If the recovery procedures are not handled appropriately, baseline ABFT will incur substantial computing overhead and contribute little to the model accuracy.

III. APPROXIMATE ABFT

In this section, we take advantage of the inherent fault tolerance of ViTs and relax the classic ABFT to an approximate

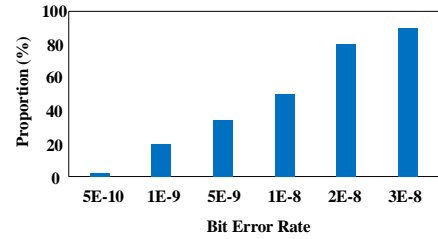


Fig. 4. The percentage of rows and columns with multiple computing errors in DeepViT-S.

ABFT, namely ApproxABFT. Since the fault tolerance capability may vary across different ViTs and different GEMMs in the same ViT, we further investigate how to approximate ABFT to fully utilize ViT fault tolerance and reduce the ABFT computing overhead and ViT accuracy loss at the same time.

A. ApproxABFT Overview

An overview of ApproxABFT is presented in Fig. 5. Unlike classical ABFT that will invoke error recovery procedures whenever computing errors are detected, ApproxABFT selectively invoke the error recovery procedures based on MSD obtained in error detection. Specifically, it relaxes the error standard and ignores computing errors that are smaller than a predefined threshold T , which greatly reduces the number of detected GEMM errors and requires much less error recovery according to the MSD error distribution shown in Fig. 3 in Section II. Similar to the error detection approximation, we also raise the R/CSD thresholds utilized to locate the computing errors in output matrix. With higher R/CSD thresholds, minor row/column deviations will be ignored and the number of computing errors to be corrected will be reduced, which can simplify the error correction. When the error location is determined, computing errors will be corrected with ABFT as much as possible. For the ones that cannot be corrected with ABFT, we further explore how to handle the computing errors to alleviate their influence on ViT accuracy.

B. Error Detection Approximation

By raising the error detection threshold in ApproxABFT, we can avoid recovering many minor computing errors that pose little influence on the model accuracy and reduce the computing overhead accordingly. However, as shown in Fig. 2, the average MSD varies across different ViT layers and we cannot utilize a single threshold to approximate error detection in different ViT layers. It remains a challenging problem to optimize the error detection threshold of different GEMMs in ViTs and minimize the ABFT computing overhead without compromising the model accuracy.

A straightforward approach is to determine the approximation threshold based on the distribution of MSD. Assume MSD of GEMMs in ViTs shows similar distribution patterns but different offsets. Then, we set a proportion threshold α for all the GEMMs in the same ViT model and the computing error occasions that $MSD \in [min, min + (max - min) \times \alpha]$ will be ignored where min and max refer to the minimum and

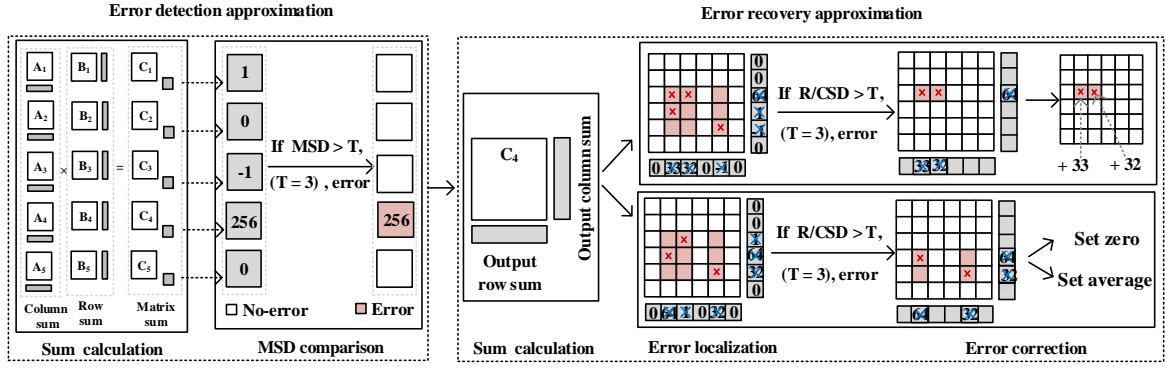


Fig. 5. ApproxABFT Overview. Different approximation strategies are applied to the error correction and error recovery procedures.

maximum values of MSD respectively. Specifically, *min* and *max* of MSD can be obtained with random fault injection to target ViT models for each BER setup. While higher α can filter out more error recovery procedures and reduce the ABFT computing overhead, it may pose more negative influence on ViT accuracy accordingly.

In this work, we optimize α with a heuristic search to compromise between model accuracy and ABFT computing overhead. We notice that ABFT protection on different GEMMs may affect each other. Basically, a GEMM with more intensive ABFT protection may alleviate the pressure of protecting the rest GEMMs given a specific accuracy constrain. To this end, we propose a heuristic GEMM-wise protection strategy to optimize the ABFT computing overhead. Specifically, we apply ABFT to a GEMM in ViT and maximize α for this GEMM as long as the model accuracy fulfills the requirement. Then, we continue the ABFT protection for the next GEMM iteratively until all the GEMMs in the ViT are protected. Since the approximation threshold α of GEMM determines the ABFT computing overhead and the computing overhead of larger GEMM is usually higher given the same error rate, we propose to apply ABFT to GEMMs in the order of GEMM sizes. Basically, larger GEMMs will be protected later when there are larger accuracy slack, which can potentially save more ABFT computing.

C. Error Recovery Approximation

As mentioned, error recovery can be split into sum calculation, error localization, and error correction. Sum calculation remains unchanged for different error recovery strategies, we mainly investigate how error localization and error correction can be approximated in this sub section.

Error localization essentially utilizes R/CSD to validate computing results in each row and each column of the output matrix. With both the error row ID and column ID, we can determine the possible faulty elements of the output matrix as shown in Fig. 5. Usually, more elements need to be corrected when there are more faulty rows and columns. Thus, we also raise the threshold of the error metric of R/CSD similar to the error detection approximation such that only significant computing errors need to be corrected. According to the two examples in Fig. 5, the number of possible faulty

elements reduces from 9 to 2 and 9 to 4 respectively with the raised thresholds, which also simplifies the following error correction procedure. As for the error threshold optimization, we follow the same approximation strategies proposed for the error detection. Although it is possible to conduct row/column-wise approximation, it can be prohibitively expensive because of the large number of rows and columns of GEMMs in a ViT model. Currently, we utilize GEMM-wise threshold optimization instead and set the same α threshold for all the rows and columns of each GEMM in ViTs.

As for the error correction, it can be divided into two different occasions as shown in Fig. 5. In the first occasion, computing errors in the output matrix can be perfectly corrected by adding the corresponding R/CSD to the faulty element when there is only one possible faulty element in a row or in a column. In the second occasion, we cannot recover the faulty elements with only R/CSD when there are more than one possible faulty elements in the corresponding rows and columns. In this case, we approximate the correction by resetting the possible faulty elements to alleviate the negative influence on the ViT accuracy. A straightforward approach is to assume the computing errors are evenly distributed and have the average R/CSD added to the possible faulty elements instead. Nevertheless, computing errors can propagate across the ViT models, average the deviation may even aggravate the error propagation. To this end, we propose to set the possible faulty elements to be zero and cut the error propagation inspired by prior fault-tolerant approaches [22].

D. ABFT Blocking

Despite the advantages of ApproxABFT, the error recovery capability remains limited especially when a GEMM is large and multiple errors may happen at the same time. Hence, applying ABFT to each GEMM in ViTs will be sub optimal. To this end, we propose to split the different GEMMs into sub GEMMs. As for the block size setups, it affects the error detection and error recovery substantially in terms of both computing overhead and recovery quality i.e. resulting model accuracy. While the recovery quality can also be adjusted with the ABFT detection and recovery thresholds, we mainly determine the block setup based on the overall ABFT computing overhead to decouple the overhead optimization

and recovery quality optimization. In general, the blocking will induce more detection overhead but potentially reduce the recovery overhead and improve the recovery quality thanks to the more fine-grained fault-tolerant processing. ApproxABFT is also revisited slightly to leverage the advantages of non-blocking and blocking. Basically, we start the error detection based on the overall GEMM. If the GEMM turns out to be fault-free, we can skip the error recovery. If faults are detected, we will further start the block-wise error detection and error recovery. Hence, the computing overhead of the block-wise ApproxABFT consists of error detection of the entire GEMM, error detection of all the sub GEMMs, and error recovery of the faulty sub GEMMs. Optimized blocking setup is determined with a heuristic search on top of fault simulation. After the blocking, we further decide the error detection and error recovery thresholds for ApproxABFT. Instead of providing unique threshold for each sub GEMMs in ViTs, we utilize the same thresholds across all the sub GEMMs to simplify the implementation. As for the implementation of the error detection and error recovery, it is the same with that illustrated in prior subsections.

IV. EXPERIMENT RESULTS

A. Experimental Setup

We select four representative ViTs models as the benchmark, including ViT-B [1], Swin-T [3], DeepViT-S [2], and CaiT-XXS-24 [4]. We take the ImageNet-1K as the dataset [23]. We utilize bit error rate (BER) to represent the bit flip error intensity and conduct the reliability analysis based on an operation-wise fault injection platform which injects random bit flip errors to outputs of the primitive operations such as addition and multiplication [21]. All the evaluation experiments are performed on a server equipped with two 24-core@2.5GHz Intel Xeon processors, 512GB memory, and four PH402 SKU 200 GPU cards.

TABLE I
SETUPS AND NOTATIONS OF DIFFERENT ABFT IMPLEMENTATIONS

	Error Detection	Error Recovery	
		Error Localization	Error Correction
BaselineABFT	BED	BEL	BEC
ApproxABFT-v1	AED	BEL	BEC
ApproxABFT-v2	AED	AEL	BEC
ApproxABFT-opt	AED	AEL	AEC

B. Overall Evaluation

We compare different ABFT approximation strategies on classical ABFT and block-wise ABFT in Fig.6 and Fig.7. For the error detection, we implemented both baseline detection (BED) and approximate detection (AED). Similarly, we implemented baseline error localization (BEL) and approximate error localization (AEL). For the error correction, B ABFT ignores the computing errors that cannot be recovered while ApproxABFT adopts approximate error correction. They are denoted as BEC and AEC respectively. As we have different approximation strategies implemented for ApproxABFT, we only utilize the optimized strategy in this experiment and detailed approximation strategies will be illustrated in Section IV-C. Specifically, we choose heuristic GEMM-wise threshold

optimization for both the error detection and error localization approximation, and we set the uncorrectable elements in the output matrix to be zero for the approximate error correction. The different ABFT setups are summarized in Table I and they are also compared with clean ViTs without errors and ViTs without protection. For the block-wise ApproxABFT, we set all the error detection and error recovery thresholds to be 10 to simplify the implementation.

The accuracy comparison shown in Fig.6 reveals that different ABFT approximation strategies implemented on classical ABFT. ApproxABFT-opt shows competitive accuracy on all the ViTs in the benchmark under various BER compared to the BaselineABFT. Particularly, the accuracy advantage is generally much more significant at higher BER. This is mainly attributed to the approximate error correction procedure because there are usually more faulty output elements at higher error rate, which is beyond the fault recovery capability of BaselineABFT. These faults can propagate along the models and aggravate on the final results, which can incur dramatic accuracy drop. When these faults are set to be zero, the error propagation is cut, which alleviates the negative influence of computing errors on ViT accuracy. In contrast, by comparing BaselineABFT, ApproxABFT-v1, and ApproxABFT-v2, we observe that the benefits of raising the threshold of error detection and error localization are mainly more significant at moderate error rate when the number of faulty elements is limited and the faults can potentially be recovered with the raised thresholds. Although the threshold induced accuracy improvement is less significant, it is critical for ApproxABFT-opt to push the resulting accuracy close to that of clean ViTs. When the proposed ABFT blocking strategy is applied, all the different ABFT optimizations including error detection approximation, error localization approximation, and error correction approximation show significant accuracy improvement under various error rate setups as presented in Fig. 7. By comparing Fig. 6 and Fig. 7, it can be observed that the approximate ABFT options especially ApproxABFT-v1 and ApproxABFT-v2 are generally sensitive to the GEMM sizes and approximate blocking enhances the overall model quality i.e. accuracy substantially.

The overhead of different ABFT implementations on classical ABFT is shown in Fig.8. Note that we take the number of multiplication operations as the computing overhead metric, but addition and comparison operations are also presented. Fig.8 shows that ApproxABFT generally reduces the computing overhead by 81.62% and 25.92% than the accurate baseline ABFT at lower BER and higher BER respectively, which is mainly attributed to the error detection approximation that reduces considerable error recovery procedures. In contrast, the approximate error recovery incurs less computing overhead and can be almost ignored compared to the total ABFT overhead. While these error recovery approximation can potentially improve the reliability of ViTs with little computing overhead, it is worthwhile to explore the different ABFT error recovery optimizations. When blocking strategy is utilized with ApproxABFT, the general trend of the different ABFT

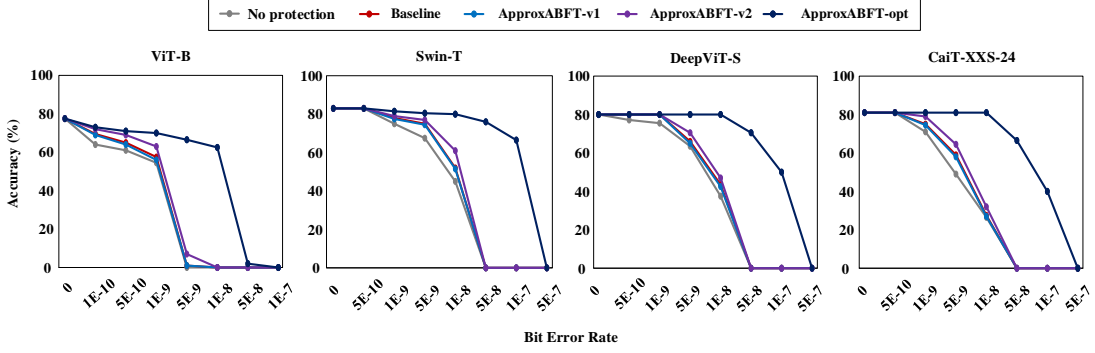


Fig. 6. Top-1 accuracy of ViTs protected with different approximation strategies on classical ABFT.

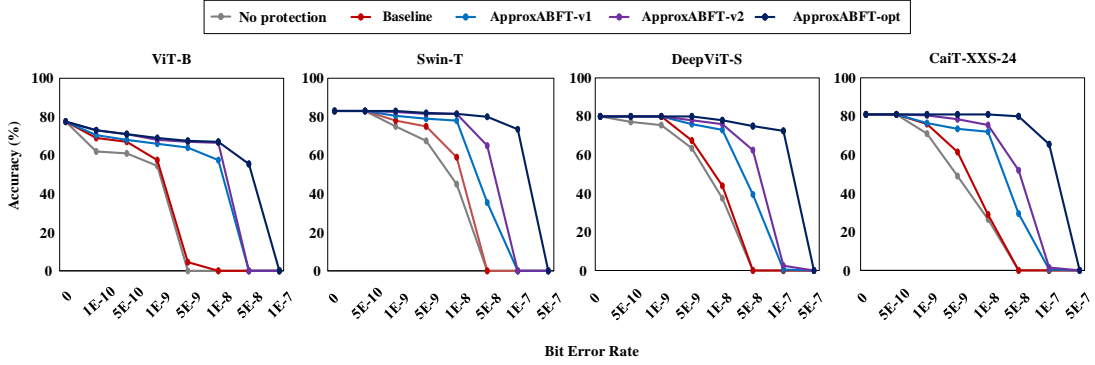


Fig. 7. Top-1 accuracy of ViTs protected with different approximation strategies on block-wise ABFT.

approximation design options remain similar but the computing overhead reduces by 6.56% to 73.5% as shown in Fig.9 compared to the corresponding non-blocking implementations. Basically, block size setup is also a key design parameter to the ABFT computing overhead.

C. Approximation Parameter Analysis

In this sub section, we take DeepViT-S as an example and explore the influence of the different design parameters of ApproxABFT on the model accuracy and ABFT computing overhead.

Since ViTs typically include a set of GEMMs, we adopt a GEMM-wise ABFT protection to fulfill the required model accuracy and minimize the computing overhead at the same time. While the order of the GEMM protection matters, we compare an in-order selection strategy and an ordered selection (ascending based on GEMM sizes) strategy used for ApproxABFT error detection and ApproxABFT error localization in Fig.10. Note that we set the model accuracy loss requirement to be no more than 1% to clean model accuracy. As shown in Fig.10 (a), the GEMM selection order in error detection of ApproxABFT has little influence on the protected model accuracy, but ascending selection consumes less computing overhead in general. It is mainly attributed to the fact that error detection over a large GEMM will be inefficient as it can invoke considerable failed error recovery procedures. Hence, the error detection with ascending order of GEMMs has less large GEMMs selected for protection given the same model accuracy requirements, which promises more efficient

ApproxABFT protection. While the error localization has little influence on the overall ApproxABFT computing overhead as discussed in prior sub section, the GEMM selection order in error localization poses little influence on computing overhead as expected and this is verified in Fig.10 (b). Nevertheless, error localization with ascending order essentially prioritizes small GEMMs and benefits the error correction, which enhances the resulting model accuracy eventually.

Thresholds are critical to the proposed ApproxABFT algorithm, and we explore the influence of different threshold setups in Fig.11. In this experiment, we have two different thresholds with fixed control parameters α as defined in Section III. Then, we have them compared with the proposed optimized blocking. For the error detection, the comparison presented in Fig.11(a) shows that all the three threshold setups can achieve similar model accuracy, but the computing overhead varies substantially. The proposed optimized blocking setup reduces the ApproxABFT computing overhead by 52.71% and 35.75% on average respectively compared to $\alpha = 4\%$ and $\alpha = 5\%$. As for the error localization, it has little influence on the overall ApproxABFT computing overhead, but it mainly affects the error recovery quality and resulting model accuracy. As shown in presented in Fig.11(b), the advantages of the optimized threshold is particularly significant at higher error rate when multiple faulty elements may occur in the same GEMM output and the number of the errors to be recovered can be reduced by the error localization approximation. In general, the proposed threshold optimization strategy can be

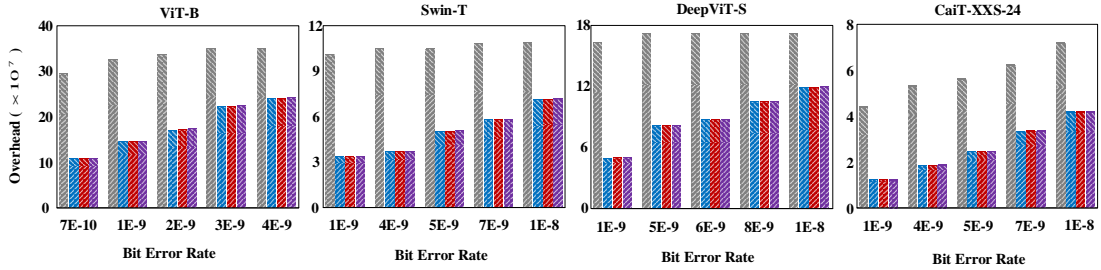


Fig. 8. Computing overhead of different ABFT implementations on classical ABFT.

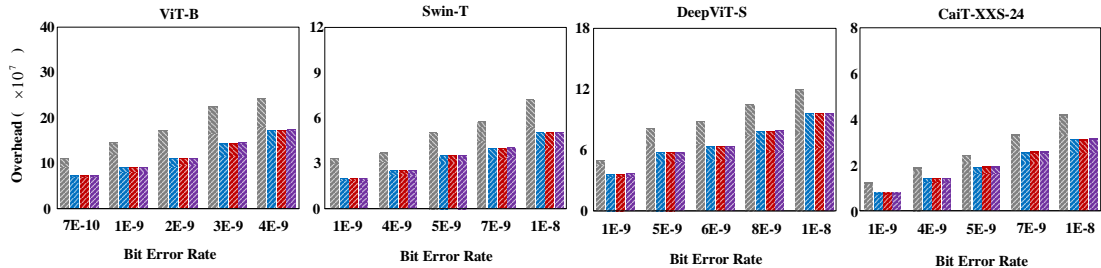
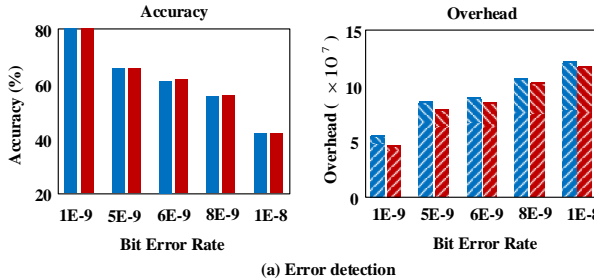
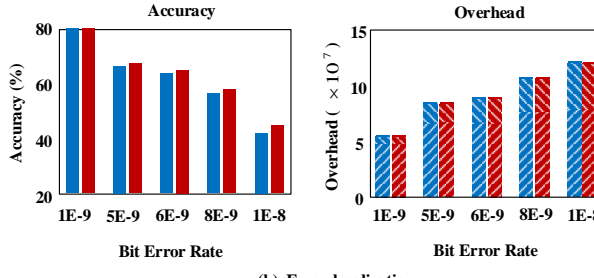


Fig. 9. Computing overhead of different ABFT implementations on block-wise ABFT.



(a) Error detection



(b) Error localization

Fig. 10. Influence of GEMM selection order in error detection and error localization of ApproxABFT.

beneficial to both the model accuracy and the computing overhead of ApproxABFT under various error rate setups.

Similar to ABFT, ApproxABFT also fails to correct multiple errors in a single GEMM precisely, but how to approximate the faulty output elements of a GEMM remains meaningful and

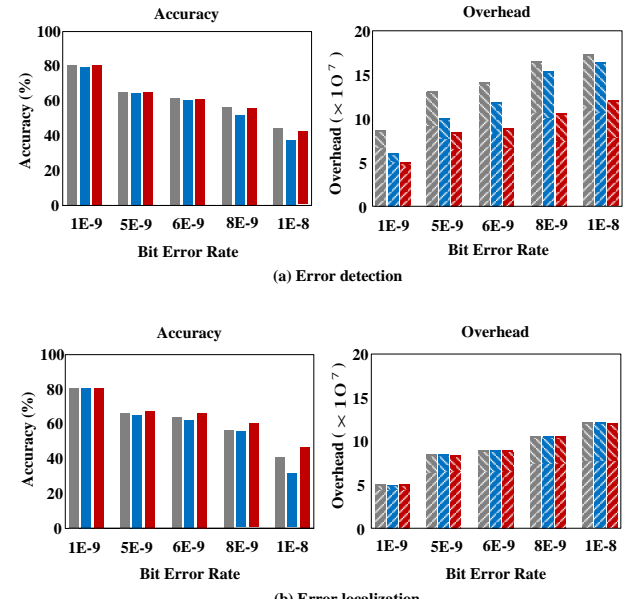
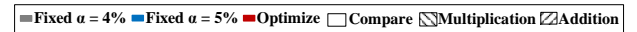


Fig. 11. Influence of error detection and error localization thresholds on ApproxABFT.

affects the resulting model accuracy. In this section, we have three different error correction strategies including Ignore, Set Average, and Set Zero compared. Basically, Ignore indicates that the faulty elements will be utilized directly. Set average utilizes the average data of a faulty region in an output array to

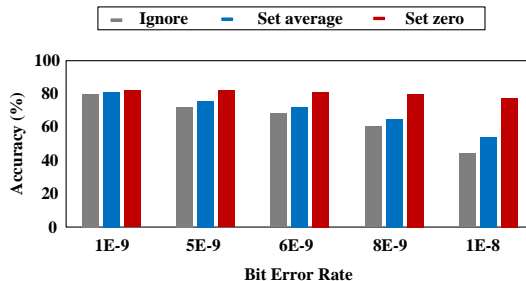


Fig. 12. Influence of different error correction strategies on ApproxABFT.

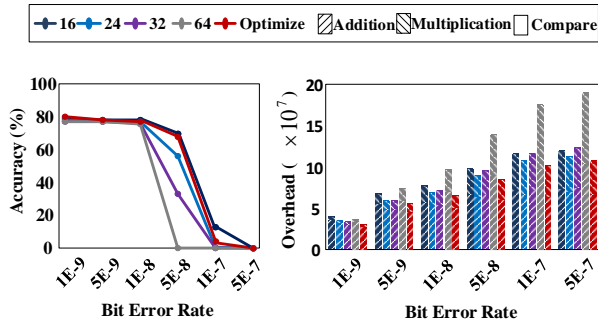


Fig. 13. Influence of block size setups on block-wise ApproxABFT.

smooth the influence of faults. Similar to set average, set zero has all the elements in a faulty region to be zero. As shown in Fig.12, set zero that essentially has the error propagation cut down greatly reduces the influence of the errors on the model and achieves higher accuracy accordingly.

As demonstrated in IV-B, block-wise ApproxABFT shows significant advantages over the non-blocking ApproxABFT in terms of both model accuracy and computing overhead. We further investigate the influence of block size setups on block-wise ApproxABFT. Suppose all the blocks are square and it is utilized across all the different GEMMs in DeepViT-S. The size of the square matrix ranges from 16 to 64. We have them implemented and compared with the optimized blocking. The comparison is presented in Fig.13. It can be seen that smaller block sizes achieve higher model accuracy in general because of the more fine-grained error detection and recovery granularity, but the advantages is trivial at relatively lower error rate when the number of faulty elements in a GEMM output matrix is limited. As for the computing overhead, optimized block size can neither be too small or too large because small blocks will induce considerable error detection overhead while large blocks can result in frequent failed error recovery procedures. However, fixed block size setups fail to adapt the GEMMs with different sizes and the proposed optimized blocking outperforms the fixed setups on both model accuracy and computing overhead.

V. RELATED WORK

The major modules like MHA and FF in ViTs can be usually implemented with GEMMs efficiently. ABFT [14] originally developed for resilient GEMMs becomes a promising approach for fault-tolerant ViTs accordingly. ABFT induced

computing patterns are generally consistent with GEMMs and the computing overhead is much less compared to classical redundancy-based approaches. Hence, it has been explored intensively for fault-tolerant design of many regular tensor-based operations such as FFT [15] [24], sparse operations [25], decomposition [26]–[28], sorting [29]. Recently, it has also been intensively explored for protecting CNNs against soft errors on various computing engines including GPUs and deep learning accelerators [16] [19] [30]. For instance, [16] leveraged the high compute-to-memory-bandwidth ratios of GPUs to reduce the execution-time overhead significantly. [19] explored the various data streams used by ABFT technology for convolution operations comprehensively. [30] proposed different check-sum strategies for deep learning models and developed customized hardware to integrate seamlessly with deep learning accelerators. However, these different approaches generally follow the accurate checksum mechanism used in traditional ABFT and can potentially benefit from the proposed approximate checksum strategy.

VI. CONCLUSION

In this work, we propose an approximate ABFT algorithm, namely ApproxABFT, based on classical ABFT for GEMMs. Instead of using strict metrics for error detection and error localization in classical ABFT, ApproxABFT relaxes the error metrics by raising the error thresholds with heuristic algorithms such that the thresholds can filter out minor computing errors and match the fault tolerance of the different GEMMs in ViTs for the sake of both higher accuracy and lower computing overhead. It is demonstrated to be beneficial to all the major ABFT procedures including error detection, error localization, and error correction. In addition, ApproxABFT also utilizes a simple yet effective zero-out approach to handle the uncorrectable computing errors and alleviate the negative influence of these errors on ViT accuracy. Finally, we also investigate influence of GEMM blocking on ApproxABFT and adapt the block size to suit GEMMs with different sizes across each ViT. According to our experiments, the proposed ApproxABFT shows significant accuracy improvement and much lower computing overhead compared to classical precise ABFT.

REFERENCES

- [1] Alexey Dosovitskiy et al. An image is worth 16x16 words: Transformers for image recognition at scale. *arXiv preprint arXiv:2010.11929*, 2020.
- [2] Daquan Zhou et al. Deepvit: Towards deeper vision transformer. *arXiv preprint arXiv:2103.11886*, 2021.
- [3] Ze Liu et al. Swin transformer: Hierarchical vision transformer using shifted windows. In *IEEE/CVF International Conf. on Computer Vision*, pages 10012–10022, 2021.
- [4] Hugo Touvron et al. Going deeper with image transformers. In *IEEE/CVF International Conf. on Computer Vision*, pages 32–42, 2021.
- [5] Yanghao Li, Hanzi Mao, Ross Girshick, and Kaiming He. Exploring plain vision transformer backbones for object detection. In *Computer Vision-ECCV 2022: 17th European Conference, Tel Aviv, Israel, October 23–27, 2022, Proceedings, Part IX*, pages 280–296. Springer, 2022.
- [6] Runsheng Xu, Hao Xiang, Zhengzhong Tu, Xin Xia, Ming-Hsuan Yang, and Jiaqi Ma. V2x-vit: Vehicle-to-everything cooperative perception with vision transformer. In *Computer Vision-ECCV 2022: 17th European Conference, Tel Aviv, Israel, October 23–27, 2022, Proceedings, Part XXXIX*, pages 107–124. Springer, 2022.

[7] Yanghao Li, Chao-Yuan Wu, Haoqi Fan, Karttikeya Mangalam, Bo Xiong, Jitendra Malik, and Christoph Feichtenhofer. Mvitv2: Improved multiscale vision transformers for classification and detection. In *Proceedings of the IEEE/CVF Conference on Computer Vision and Pattern Recognition*, pages 4804–4814, 2022.

[8] Zhenda Xie, Zheng Zhang, Yue Cao, Yutong Lin, Jianmin Bao, Zhuliang Yao, Qi Dai, and Han Hu. Simmim: A simple framework for masked image modeling. In *Proceedings of the IEEE/CVF Conference on Computer Vision and Pattern Recognition*, pages 9653–9663, 2022.

[9] Eshagh Kargar et al. Vision transformer for learning driving policies in complex multi-agent environments. *Preprint arXiv:2109.06514*, 2021.

[10] Robert E Lyons and Wouter Vanderkulk. The use of triple-modular redundancy to improve computer reliability. *IBM journal of research and development*, 6(2):200–209, 1962.

[11] Dawen Xu, Meng He, Cheng Liu, Ying Wang, Long Cheng, Huawei Li, Xiaowei Li, and Kwang-Ting Cheng. R2f: A remote retraining framework for aiot processors with computing errors. *IEEE Transactions on Very Large Scale Integration (VLSI) Systems*, 29(11):1955–1966, 2021.

[12] Hossein Sayadi et al. A data recomputation approach for reliability improvement of scratchpad memory in embedded systems. In *IEEE International Symposium on DFT in VLSI and Nanotechnology Systems*, pages 228–233. IEEE, 2014.

[13] Shanshan Liu, Pedro Reviriego, Xiaochen Tang, Wei Tang, and Fabrizio Lombardi. Result-based re-computation for error-tolerant classification by a support vector machine. *IEEE Transactions on Artificial Intelligence*, 1(1):62–73, 2020.

[14] Kuang-Hua Huang et al. Algorithm-based fault tolerance for matrix operations. *IEEE Trans. on computers*, 100(6):518–528, 1984.

[15] Sying-Jyan Wang and Niraj K. Jha. Algorithm-based fault tolerance for fft networks. *IEEE Transactions on Computers*, 43(7):849–854, 1994.

[16] Jack Kosaian and KV Rashmi. Arithmetic-intensity-guided fault tolerance for neural network inference on GPUs. In *International Conf. for HPC, Networking, Storage and Analysis*, pages 1–15, 2021.

[17] Siva Kumar Sastry Hari, Michael B Sullivan, Timothy Tsai, and Stephen W Keckler. Making convolutions resilient via algorithm-based error detection techniques. *IEEE Transactions on Dependable and Secure Computing*, 19(4):2546–2558, 2021.

[18] Shixun Wu, Yujia Zhai, Jinyang Liu, Jiajun Huang, Zizhe Jian, Bryan M Wong, and Zizhong Chen. Anatomy of high-performance gemm with online fault tolerance on gpus. *arXiv preprint arXiv:2305.01024*, 2023.

[19] Kai Zhao et al. Ft-cnn: Algorithm-based fault tolerance for convolutional neural networks. *IEEE Trans. on Parallel and Distributed Systems*, 32(7):1677–1689, 2020.

[20] J Chen et al. Gpu-abft: Optimizing algorithm-based fault tolerance for heterogeneous systems with gpus. In *2016 IEEE International Conf. on NAS*, pages 1–2, 2016.

[21] Xinghua Xue et al. Winograd convolution: A perspective from fault tolerance. In *59th ACM/IEEE DAC*, pages 853–858, 2022.

[22] Jeff Jun Zhang et al. Fault-tolerant systolic array based accelerators for deep neural network execution. *IEEE Design & Test*, 36(5):44–53, 2019.

[23] Jia Deng et al. Imagenet: A large-scale hierarchical image database. In *2009 IEEE Conf. on CVPR*, pages 248–255, 2009.

[24] Xin Liang, Jieyang Chen, Dingwen Tao, Sihuan Li, Panruo Wu, Hongbo Li, Kaiming Ouyang, Yuanlai Liu, Fengguang Song, and Zizhong Chen. Correcting soft errors online in fast fourier transform. In *Proceedings of the International Conference for High Performance Computing, Networking, Storage and Analysis*, pages 1–12, 2017.

[25] Alexander Schöll et al. Efficient algorithm-based fault tolerance for sparse matrix operations. In *46th Annual IEEE/IFIP International Conf. on DSN*, pages 251–262. IEEE, 2016.

[26] Panruo Wu et al. Towards practical algorithm based fault tolerance in dense linear algebra. In *25th ACM International Symposium on High-Performance Parallel and Distributed Computing*, pages 31–42, 2016.

[27] Jieyang Chen, Hongbo Li, Sihuan Li, Xin Liang, Panruo Wu, Dingwen Tao, Kaiming Ouyang, Yuanlai Liu, Kai Zhao, Qiang Guan, et al. Fault tolerant one-sided matrix decompositions on heterogeneous systems with gpus. In *SC18: International Conference for High Performance Computing, Networking, Storage and Analysis*, pages 854–865. IEEE, 2018.

[28] Quang Minh Nguyen, Haewon Jeong, and Pulkit Grover. Coded qr decomposition. In *2020 IEEE International Symposium on Information Theory (ISIT)*, pages 191–196. IEEE, 2020.

[29] Sihuan Li et al. Ft-isort: Efficient fault tolerance for introsort. In *International Conf. for High Performance Computing, Networking, Storage and Analysis*, pages 1–17, 2019.

[30] Elbruz Ozen and Alex Orailoglu. Sanity-check: Boosting the reliability of safety-critical deep neural network applications. In *2019 IEEE 28th ATS*, pages 7–75, 2019.